SLAC-PUB-5258
June 1990
E/T

Measurement of the W^+W^- Threshold*

MORRIS L. **SWARTZ**

Stanford Linear Accelerator Center
Stanford University, Stanford, California 94309

ABSTRACT

Scan strategies for the measurement of the $e^+e^- \rightarrow W^+W^-$ threshold are discussed. The most sensitive beam energies (E_b) for the measurement of the W mass (M_W) and width (Γ_W) are $E_b \simeq M_W$ + 0.5 GeV and $E_b \simeq M_W - 1$ GeV, respectively. With a commitment of 250 pb^{-1} to the measurement of the W-pair threshold, it appears to be possible measure M_W with a precision $\delta M_W \lesssim 160$ MeV. The corresponding precision on the width, $\delta\Gamma_W$ = 400-500 MeV, is not competitive with recent indirect determinations from the CDF and UA2 collaborations.

Submitted to Nuclear *Physics B*

⋆**Work** supported by the Department of Energy, contract DE--AC03--76SF00515.

1. Introduction

The recent precise measurements[1] of the mass of the Z^0 boson (M_Z) have completed the tree-level specification of the electroweak parameters of the Standard Model. Precise measurements of other physical quantities that are related to the electroweak parameters *test the Standard Model* at the loop level. A precise measurement of the W boson mass (M_W) will be an important contribution to this field.

Currently, the most precise determination of M_W is extracted from the measurement of the ratio M_W/M_Z by the UA2 Collaboration at the $S p\bar{p}S$ collider,[2]

$$M_W = \text{SO.49} \pm 0.43(\text{stat}) \pm 0.24(\text{syst})\ \text{GeV}.$$

Future work at the Tevatron collider may improve the precision of this type of measurement to the level δM_W = 100-200 MeV.

The production of W boson pairs will become possible in the second phase of LEP operation. The installation of superconducting RF cavities will permit the beam energy to be increased to a value above the threshold for the process $e^+e^- \rightarrow W^+W^-$. The main focus of the LEP200 physics program will be to study the three gauge boson vertex. It will also be possible to perform measurements of the mass and width of the W boson.

There are several different techniques that can be used to perform these measurements. It is possible to extract M_W from measurements of the W pair threshold shape and from measurements of the distributions of jet masses and lepton energies. These methods are are described in Reference 3.

The purpose of this document is to consider scan strategies that are necessary for the optimization of the threshold measurement. The small absolute size of the W pair cross section implies that the threshold measurement will be limited by event statistics. It will be desirable to use the available luminosity in an optimal manner.

2. High Energy e^+e^- Cross Sections

The character of the total e^+e^- cross section in the region of the W pair threshold differs somewhat from the more familiar region of center-of-mass energy $\sqrt{s} < M_Z$.

2.1. THE CROSS SECTION FOR $e^+e^- \rightarrow f\bar{f}$

The basic $e^+e^- \rightarrow f\bar{f}$ cross section for five quark and three lepton flavors increases from about 7 units of R at center-of-mass energies below the Z^0 pole to 10 units of R at energies above the Z^0 pole. The tree-level cross section is approximately 34 pb at $\sqrt{s}$ = 160 GeV. Unfortunately, the initial state radiative corrections increase this number enormously. The cross section for the process $e^+e^- \rightarrow \gamma Z^0$ is approximately three times larger than the high mass neutral current cross section. This is illustrated in Figure 1. The cross section for $e^+e^- \rightarrow f\bar{f}(\gamma)$ is plotted as a function of the normalized $f\bar{f}$ longitudinal momentum x_F and of the $f\bar{f}$ center-of-mass energy $E_{f\bar{f}}$. The center-of-mass energy of the e^+e^- system $\sqrt{s}$ is 160 GeV. Note that there is a large peak near the nominal center-of-mass energy $E_{f\bar{f}} \simeq \sqrt{s}$ and x_F = 0 and two larger peaks near $E_{f\bar{f}} = M_Z$ and $x_F = \pm 0.68$. The latter peaks correspond to highly boosted Z^0 bosons. At $\sqrt{s}$ = 160 GeV, we estimate the size of the total cross section to be -150 pb.

2.2. THE W^+W^- CROSS SECTION

The tree-level cross section for the process $e^+e^- \rightarrow W^+W^-$ has been calculated by Muta, Najima, and Wakaizumi.[4] They incorporate the finite width of the W by expressing the cross section in the following form,

$$a_{,,}(s) = \int_0^s ds_1 \rho(s_1) \int_0^{(\sqrt{s}-\sqrt{s_1})^2} ds_2 \rho(s_2) \sigma(s, s_1, s_2), \qquad (1)$$

where: s is the square of the center-of-mass energy; s_1 and s_2 are the squares of the invariant masses of the W bosons; $\sigma(s, s_1, s_2)$ is the tree-level cross section for

the production of W bosons of masses $\sqrt{s_1}$ and $\sqrt{s_2}$; and the function p(s) is a normalized Breit-Wigner distribution function,

$$\rho(s) = \frac{1}{\pi M_W} \cdot \frac{s\Gamma_W}{(s - M_W^2)^2 + s\Gamma_W^2},$$

where Γ_W is the W boson width.

We incorporate initial state radiation into the calculation using the structure function approach of Nicrosini and Trentadue,[5]

$$\sigma_{ww}(s) = \int dx_1 dx_2 D(x_1, s) D(x_2, s \int_0^A) \qquad ds \int_0^B \rho(s_1)\, ds_2 \rho(s_2) \sigma(x_1 x_2 s, s_1, s_2), \quad (2)$$

where $D(x, s)$ is the electron structure function and A, B are limits: $A = x_1 x_2 s$, $B = (\sqrt{x_1 x_2 s} - \sqrt{s_1})^2$.

The cross section $\sigma(s, s_1, s_2)$ has contributions from s-channel photon and Z^0 subprocesses and a t-channel neutrino subprocess. The form of the cross section is too complex to reproduce here and the reader is referred to Appendix A for the gory details. The result of the four-dimensional integration given in equation (2) is plotted in Figure 2 as a function of $E_b - M_W$ where E_b is the single beam energy. The mass and width of the W are assumed to be 80 GeV and 2.1 GeV, respectively. Note that three curves are plotted: the dashed curve is the basic tree-level cross section; the dashed-dotted curve is the cross section including the effect of initial state radiation; and the solid curve is the cross section including initial state radiation and the effect of a finite W width. The inclusion of initial state radiation reduces the size of the cross section. The finite W width produces non-zero cross section at energies below the nominal threshold at $E_b = M_W$.

3. Scanning Theory

The optimization of a threshold or resonance scan requires some a *priori* knowledge of the lineshape to be measured. In this case, the W mass has been measured to some reasonable accuracy and the Standard Model predicts the threshold shape in terms of several parameters (M_W and Γ_W).

Let us consider a hypothetical scan of N energy-luminosity points:

$$E_b = E_1, E_2, \ldots . E_N$$
$$\int \mathcal{L} dt = L_1, L_2, \ldots . L_N.$$

We assume that a cross section σ_i is measured at each point,

$$\sigma_{measured} = \sigma_1, \sigma_2, ..., \sigma_N.$$

The M parameters a_j $(j = 1, M)$ of our theoretical lineshape $o(E)$ can be extracted from a χ^2 fit to the measured points. The quantity χ^2 is defined as,

$$\chi^2 \equiv \sum_{i=1}^{N} \frac{[\sigma_i - \sigma(E_i)]^2}{(\delta\sigma_i)^2}, \tag{3}$$

where $\delta\sigma_i$ is the error on the i^{th} measurement.

The best estimate of the parameters $(\bar{a}_j)$ is the one that minimizes χ^2. The parameter errors are found from a Taylor expansion of χ^2 about the minimum value,

$$\begin{aligned} \chi^2 &= \chi^2(\bar{a}) + \frac{1}{2} \sum_{j\,k=1}^{M} \frac{\partial^2 \chi^2}{\partial a_j \partial a_k} (a_j - \bar{a}_j)(a_k - \bar{a}_k) \\ &= \chi^2(\bar{a}) + \sum_{j,k=1}^{M} (\mathbf{C}^{-1})_{jk} (a_j - \bar{a}_j)(a_k - \bar{a}_k) \end{aligned}, \tag{4}$$

where the matrix $\mathbf{C}^{-1}$ is the inverse of the parameter covariance matrix. The error hyperellipsoid is determined by changing χ^2 by one unit about the minimum value.

It is straightforward to show that the parameter errors are given by the diagonal elements of the covariance matrix C,

$$(\delta a_j)^2 = \mathbf{C}_{jj}. \tag{5}$$

Averaging equation (4) over many experiments, the inverse matrix can be expressed in the following form,

$$(\mathbf{C}^{-1})_{jk} = \sum_{i=1}^{N} \frac{1}{(\delta\sigma_i)^2} \cdot \left[\frac{\partial\sigma}{\partial a_j}(E_i)\right] \cdot \left[\frac{\partial\sigma}{\partial a_k}(E_i)\right]. \tag{6}$$

Although equation (6) is quite general, it is useful to express the cross section errors in terms of the luminosity and the theoretical cross section. Ignoring the statistical errors on the luminosity measurements: we can express the cross section errors as $(\delta\sigma_i)^2 = \sigma(E_i)/L_i$. Equation (6) can then be written as,

$$(\mathbf{C}^{-1})_{jk} = \sum_{i=1}^{N} \frac{L_i}{\sigma(E_i)} \cdot \frac{\partial\sigma}{\partial a_j}(E_i) \cdot \frac{\partial\sigma}{\partial a_k}(E_i) = \sum_{i=1}^{N} L_i \cdot S(E_i, a_j) \cdot S(E_i, a_k), \tag{7}$$

where we define the so-called sensitivity *function* $S(E, a_j)$ as

$$S(E, a_j) \equiv \frac{1}{\sqrt{\sigma(E)}} \cdot \frac{\partial\sigma}{\partial a_j}(E). \tag{8}$$

If the lineshape is a function of a single parameter or if the off-diagonal elements of the inverse matrix $\mathbf{C}^{-1}$ are small, the parameter errors have a particularly simple form,

$$(\delta a_j)^{-2} \simeq \sum_{i=1}^{N} L_i \cdot \left[S(E_i, a,)\right]^2. \tag{9}$$

Equation (9) implies that the error δa_j is minimized when the integrated luminosity is concentrated in regions of *scan energy where $|S(E, a_j)|$ is large.* Note that $|S(E, a_j)|$ is lar g where the derivative $|\partial\sigma/\partial a_j|$ is 1arge and where the cross section is small.

★ This assumption is quite valid for the measurement of non-resonant cross sections.

The correlations between the parameters are described by the off-diagonal elements of the matrices $\mathbf{C}^{-1}$ and C (the error ellipsoid is unrotated if they vanish). *The presence of non-zero correlation always increases a parameter error beyond the value given in equation* (9).† It is clearly important to minimize the off-diagonal elements by our choice of the scan point luminosities.

Equations (7) and (5) predict the complete parameter error matrix in terms of the theoretical lineshape and the scan point luminosities. *Note that it is assumed that* χ^2 *is well-defined* ($N > M$) *and that a sufficient number of events is collected at each point that the errors* are *Gaussian.*

Since any cross section measurement has an associated normalization uncertainty, it is important to consider the sensitivity of the final result to systematic shifts in the measured cross sections. Expanding the theoretical cross section in parameter space about the best estimates $\bar{a}_j$, it is straightforward to derive the average shift in a parameter Δa_j caused by shifts in the measured cross sections $\Delta\sigma_i$,

$$\langle \Delta a_j \rangle = \sum_{k=1}^{M} \mathrm{C}_{jk} \cdot \sum_{i=1}^{N} L_i \cdot \frac{\Delta\sigma_i}{\sigma_i} \cdot \frac{\partial\sigma}{\partial a_k}(E_i). \tag{10}$$

It is clear that we would like to choose the energies and luminosities to minimize the parameter errors and the correlations between the parameters. We can be guided in this task by examining the energy dependence of the functions $S(E, a_j)$.

† The presence of non-zero correlation allows the error associated one parameter to leak into the error associated with another parameter.

4. Mass and Width of the W

It was shown in chapter 2 that the total e^+e^- cross section in the region of the W-pair threshold is dominated by the ordinary $f\bar{f}(\gamma)$ final state: The isolation of the W-pair signal requires the application of some selection criteria. The measured cross section therefore has the following form,

$$\sigma_{meas}(E_b) = \varepsilon_{ww}\sigma_{ww}(E_b) + \frac{B}{(2E_b)^2}, \tag{11}$$

where: ε_{ww} is the efficiency to identify a W-pair event; $\sigma_{ww}(E_b)$ is the cross section plotted in Figure 2; and B is a constant that represents the residual background (which presumably scales as 1/s).

The sensitivity function for some parameter a_j of the W^+W^- cross section therefore has the following form,

$$S(E, a_j) = \frac{\varepsilon_{ww}}{\sqrt{\varepsilon_{ww}\sigma_{ww}(E_b) + B/(2E_b)^2}} \cdot \frac{\partial\sigma_{ww}}{\partial a_j}(E_b). \tag{12}$$

The cross section σ_{ww} and its derivatives* with respect to M_W and Γ_W are tabulated as functions of $\epsilon_b = E_b - M_W$ in Table I (assuming parameter values: M_W = 80 GeV, Γ_W = 2.1 GeV). The mass and width derivatives peak at points of small cross section (5.0 pb and 2.1 pb, respectively). The total cross section in this region is larger than 150 pb and the large $E_{f\bar{f}}$ cross section is 35-40 pb. It is clear from equation (12) that any selection criteria that can reduce the background to a level that is comparable to or smaller than the W pair cross sections are worth a modest price in detection efficiency.

---

* The calculation of the derivative $da_{ww}/\partial M_W$ assumes that the weak coupling g does not vary with M_W. See Appendix A for a more complete discussion.

4.1. SELECTION CRITERIA

The background processes produce mostly two- and three-jet hadronic events or lepton pair events that are often highly boosted along the beam direction. The visible energy of the background is often small as compared with $2E_b$. The W-pair events appear most often as four-jet events (-44% of W-pairs) or as an energetic lepton and two jets (-44% of IV-pairs).

-The authors of Reference 3 have studied a number of selection criteria to reduce the background cross section to less than -1 pb while retaining -75% of the four-jet and $\sim 45\%$ of the lepton+two-jet events (we assume that τ leptons cannot be used and that one third of the remaining events are eliminated by the isolation cut used to suppress heavy flavor events). The net efficiency for the detection of W-pair events is therefore $\varepsilon_{ww} \simeq 0.53$.† Note that the sensitivity functions $|S(E_b, M_W)|$ and $|S(E_b, \Gamma_W)|$ are increased greatly by the application of these criteria (see equation (12)).

4.2. THE SENSITIVITY FUNCTIONS

The results of the last section can be used to calculate the sensitivity functions for a real measurement of the W-pair threshold. We assume that the efficiency is ε_{ww} = 0.53 and that the residual background is 1 pb at $E_b = M_W$ (we take the constant B in equation (11) to be B = 1 pb . $(2M_W)^2$). It is then straightforward to calculate the sensitivity functions for M_W, Γ_W, and the background constant B.

The sensitivity function $S(E_b, M_W)$ is plotted in Figure 3 as a function of $\epsilon_b = E_b - M_W$. Note that the maximum sensitivity occurs at $\epsilon_b \simeq 0.5$ GeV.

The sensitivity function $S(E_b, \Gamma_W)$ is shown in Figure 4 as a function of ϵ_b. As one would expect, it peaks just below the nominal threshold (ϵ_b = -1 GeV) where

† The W^+W^- final state that consists of a pair of monochromatic acoplanar charged leptons can presumably be separated from the background with some efficiency. Our estimate of ε_{ww} is therefore somewhat conservative.

the width-induced *tail* in the cross section is largest. The function $S(E_b, \Gamma_W)$ decreases rapidly as E_b is increased. It passes through zero near ϵ_b = 1 GeV and plateaus above ϵ_b = 3 GeV. The sensitivity in the plateau region is due to the reduction in the cross section caused by the finite width (see Figure 2). The maximum value of $|S(E_b, \Gamma_W)|$ is smaller than the maximum value of the mass sensitivity function by a factor of three. A good measurement of Γ_W will clearly require a substantial commitment of luminosity to a point of very small cross section. Note that the product $S(E_b, M_W)$. $S(E_b, \Gamma_W)$ is an odd function about the point ϵ_b = 1 GeV. In principle, the M_W-Γ_W correlation can be cancelled by measuring the cross section on both sides of this point. The functions $S(E_b, M_W)$ and $S(E_b, \Gamma_W)$ are not large in the region ϵ_b > 1 GeV. The cancellation of the correlation therefore requires a substantial commitment of luminosity to a relatively insensitive region.

The function $S(E_b, B)$ is plotted as a function of ϵ_b in Figure 5. As one would expect, the background sensitivity is largest at small beam energy and decreases dramatically as E_b increases through the W pair threshold. Note that it is possible to cancel the B-Γ_W correlation but that it is not possible to cancel the B-M_W correlation.

4.3. SCAN STRATEGIES

It is clear that precise measurements of M_W and Γ_W require that LEP be operated in regions of small cross section. Since all other studies of the W-pair system require a large sample of data, there will be considerable pressure to operate the machine on the cross section plateau at the largest available energy. In order to estimate how precisely M_W and Γ_W could be measured in a l-2 year run (500 pb^{-1}), we assume that 50% of the luminosity is dedicated to operating at the largest available energy (we assume that ϵ_b = 15 GeV or $\sqrt{s}$ = 190 GeV is achieved) and the remaining 50% is dedicated to operation in the threshold region.

It is instructive to first consider an extremely unrealistic scan scenario. We assume that we will measure only one parameter and that the other parameters

are precisely known. In this case, we need only one scan point in the threshold region for a constrained fit. We choose to allocate the entire 250 pb^{-1} luminosity to operation at the most mass-sensitive point (ϵ_b = 0.5 GeV) or at the most width-sensitive point (ϵ_b = -1 GeV). Using equation (9) we estimate the precision of these measurements to be

$$\delta M_W = 92 \text{ MeV or } \delta\Gamma_W = 286 \text{ MeV}.$$

The M_W measurement would be a very desirable result. The Γ_W measurement is not competitive with the recent indirect determinations that have been published by the CDF and UA2 collaborations,[6,7]

$$\Gamma_W = (0.85 \pm 0.08) \cdot \Gamma_Z = 2.19 \pm 0.20 \text{ GeV (CDF)}$$
$$\Gamma_W = (0.89 \pm 0.08). \Gamma_Z = 2.30 \pm 0.20 \text{ GeV (UA2)}.$$

Since the width cannot be measured to an interesting level, it is clearly unwise to design a scan to measure Γ_W. We therefore concentrate on the measurement of M_W.

A real measurement of M_W will require that the background constant B be varied as a fit parameter. Unfortunately, the B-M_W correlation cannot be canceled by a clever choice of scan points. It is therefore necessary to measure both parameters well.

The number of scan points is somewhat arbitrary. A minimum of three points are required to constrain the two parameter problem. The presence of a high energy point implies that only two points are needed in the threshold region. Equation (7) implies that several closely spaced points in a region of large sensitivity are equivalent to a single point in the same region. We can therefore analyze the optimization of the M_W measurement by considering a two-point threshold measurement.

An optimal scan must include an energy point in a region of large background sensitivity $|S(E_b, B)|$ and one near the maximum of the mass sensitivity function $|S(E_b, M_W)|$. We choose the scan point energies to be ϵ_b = -5 GeV and

ϵ_b = 0.5 GeV, respectively.* The apportionment of the available luminosity between the two points is a straightforward problem in one-dimensional optimization. We find that the error δM_W has a very broad minimum about the ratio of luminosities, $L(0.5\ \mathrm{GeV})/L(-5\ \mathrm{GeV}) \simeq 2/1$. If the luminosities of the -5 GeV and 0.5 GeV points are 85 pb^{-1} and 165 pb^{-1}, respectively, the minimum value of the error δM_W is approximately 155 MeV.

A two-point threshold scan is somewhat risky. It is safer to bracket the region of maximum M_W sensitivity with several scan points. We therefore construct an optimal four-point scan (a five-point measurement when the ϵ_b = 15 GeV point is included) by assigning one third of the 165 pb^{-1} (55 pb^{-1}) to each of three points: ϵ_b = 0 GeV, 0.5 GeV, and 1.0 GeV. It is instructive to compare this scan (Scan 1) with a slightly modified version. The modified version (Scan 2) is created by shifting the luminosity from the ϵ_b = 0 GeV point to ϵ_b = -1 GeV. We expect the second scan strategy to improve the width measurement at the expense of the mass measurement. Finally, we note that our modified scan strategy is similar to the scan strategy that was studied in Reference 3 (which we label Scan 3). The authors of Reference 3 assigned 100 pb^{-1} to each of the following five points: ϵ_b = -5 GeV, -1 GeV, 0 GeV, 1 GeV, and 15 GeV.

Using equation (7) and the sensitivity functions, the performance of each scan scenario can be estimated. The expected number of detected events and the expected precisions δM_W, $\delta \Gamma_W$, and δB are listed in Table II for each of the three scan strategies. The presence of a high energy point in each strategy reduces the M_W-Γ_W correlation sufficiently that the M_W precision obtained from the three parameter fit is essentially identical to that obtained from a two-parameter fit.

As one might expect, the third scan strategy which allocates 400 pb^{-1} to the threshold measurement provides the most precise M_W measurement, δM_W = 150 MeV. *The M_W precision obtained from the optimized mass scan (Scan 1) is*

* Varying the energy of the second point about ϵ_b = 0.5 GeV verifies that the B-M_W correlation does not shift the point of maximum M_W sensitivity.

worse by 7%. Note however, that Scan 1 produces nearly GO% more events than does Scan 3. Surprisingly, the second scan strategy provides a slightly better width measurement than does the third strategy. This occurs because the second scan produces a smaller B-Γ_W correlation than does the third scan strategy.

It is clear from equation (12) that the functions $S(E_b, a_j)$ are sensitive to the level of residual background and to the W-pair detection efficiency. We investigate these effects by reducing the background constant to B = 0.5 pb . $(M_W)^2$ and by-increasing the detection efficiency to ε_{ww} = 0.70. The results are listed in Table II. The error δM_W is improved by approximately 20 MeV in the case that the background is reduced by a factor of two. The mass error is improved by approximately 30 MeV when the efficiency is increased. Note that the optimal luminosity ratio L(0.5 GeV)$/L(-5$ GeV) is nominally sensitive to both effects. However, the optimal region is so broad that the use of a $2/1$ ratio degrades the result by less than 1%.

4.4. SYSTEMATIC ERRORS

The measurement of the W-pair threshold is affected by systematic uncertainties on the energy scale and cross section normalization. The energy scale uncertainty affects the M_W measurement directly. Assuming that the fractional error on the beam energy scale is constant, the uncertainty on M_W should be comparable to the one that applies to the M_Z measurement. By 1994, this uncertainty is expected to be -20 MeV.

The sensitivity of the results given in Table II to normalization errors can be estimated from equation (10). Taking the first scan strategy as an example, we estimate that the uncertainties on the parameters are related to an overall normalization uncertainty $\delta\sigma/\sigma$ as follows,

$$\delta M_W = -\ 2.26\ \text{GeV} \cdot \frac{\delta\sigma}{\sigma}$$

$$\delta\Gamma_W = -\ 19.3\ \text{GeV} \cdot \frac{\delta\sigma}{\sigma}.$$

The normalization error must be controlled to the 3% level to avoid inflating the M_W error.

4.5. SENSITIVITY TO ASSUMPTIONS

Our analysis assumes that we have complete *a priori* knowledge of the W resonance parameters. Although the characteristic width in E_b space of the M_W-sensitive region is larger than the current uncertainty on M_W, our precision estimates are likely to be somewhat optimistic. It is possible to alter the results by $\lesssim 10\%$ by varying the resonance parameters over reasonable intervals.

5. Conclusions

Despite the uncertainties on the ultimate W-pair detection efficiency and residual background contamination, several conclusions can be drawn from this analysis:

1. The most sensitive scan region for the measurement of M_W is ϵ_b = O-l GeV. *The mapping of the entire threshold shape would produce a less precise measurement.*

2. It is not possible to remove the correlation between the background parameter and M_W by a clever choice of scan point energies. This implies that a scan point of energy below the nominal threshold is quite important. If the energy is chosen to be ϵ_b = -5 GeV (E_b = 75 GeV), an M_W-optimized scan strategy would allocate twice as much integrated luminosity to the M_W sensitive region as is allocated to the low energy point.

3. A measurement of M_W at the $\lesssim 160$ MeV level is possible with the dedication of a large integrated luminosity (250 pb^{-1}) and good control of the background contamination.

4. The measurement of Γ_W to an interesting level is difficult or impossible. It is probably unwise to attempt anything more than a cursory measurement.

Acknowledgements:

The author would like to thank Gary Feldman and Michael Peskin for useful conversations.

REFERENCES

1. G. Abrams et al., *Phys. Rev. Lett. 63* (1989) 2173;
   D. Decamp et al., *Phys. Lett.* **B231** (1989) 519 and *Phys. Lett.* **B235** (1990) 399;
   P. Aarnio et al., *Phys. Lett.* **B231** (1989) 539;
   B. Adeva et al., *Phys. Lett.* **B231** (1989) 509 and L3 Preprint #004, December 1989;
   M.Z. Akrawy et al., *Phys. Lett.* **B231** (1989) 530.
2. J. Alitti et al., CERN preprint CERN-EP/90-22, March 1990.
3. J. Bijnens et al., *Proceedings of the ECFA Workshop on LEP 200*, edited by A. Böhm and W. Hoogland, CERN 87-08, June 1987, pg 85.
4. T. Muta, R. Najima, and S. Wakaizumi, *Mod. Phys. Lett.* **Al** (1986) 203.
5. 0. Nicrosini and L. Trentadue, *Phys. Lett.* **185B** (1987) 395.
6. F. Abe et al., *Phys. Rev. Lett.* **62** (1990) 154.
7. J. Alitti et al., CERN preprint CERN-EP/90-20, February 1990.

Table I

The W-pair cross section and its derivatives as functions of beam energy $\epsilon_b = E_b - M_W$. The W mass and width are assumed to be SO GeV and 2.1 GeV, respectively. The errors are the statistical -uncertainties associated with the Monte Carlo integration.

ϵ_b (GeV)	σ_{ww} (Pb)	$\partial\sigma_{ww}/\partial M_W$ (pb/GeV)	$\partial\sigma_{ww}/\partial\Gamma_W$ (pb/GeV)
-5.0	0.44f0.01	-0.102f0.004	0.195f0.005
-4.0	0.56f0.01	-0.153f0.005	0.241f0.004
-3.5	0.59f0.01	-0.188±0.005	0.275f0.004
-3.0	0.6Sf0.01	-0.239f0.006	0.318±0.004
-2.5	0.84±0.02	-0.310f0.006	0.375f0.005
-2.0	1.00f0.02	-0.407f0.007	0.424f0.005
-1.5	1.23f0.02	-0.591±0.008	0.500f0.005
-1.0	1.56f0.02	-0.859±0.010	0.567f0.006
-0.5	2.09f0.03	-1.34f0.01	0.603f0.006
0.0	2.91f0.03	-1.91f0.01	0.491f0.007
0.5	3.87±0.03	-2.27±0.02	0.223±0.008
1.0	5.01f0.04	-2.29f0.02	-0.026f0.010
1.5	5.99f0.05	-2.17f0.02	-0.215f0.011
2.0	6.99f0.05	-2.05±0.02	-0.336f0.012
2.5	7.81±0.05	-1.88±0.03	-0.415f0.013
3.0	S.59f0.06	-1.78±0.03	-0.464f0.014
3.5	9.42f0.06	-1.67±0.03	-0.501f0.015
4.0	10.06f0.07	-1.50f0.03	-0.546f0.016
4.5	10.55f0.07	-1.48±0.03	-0.533f0.016
5.0	11.19f0.07	-1.43f0.03	-0.573f0.017
5.5	11.65f0.07	-1.34f0.04	-0.550f0.017
6.0	12.18±0.08	-1.29f0.04	-0.567±0.018
7.0	12.96±0.08	-1.19f0.04	-0.537f0.020
8.0	13.59±0.08	-1.01±0.04	-0.571f0.020
10.0	14.74f0.09	-0.902f0.043	-0.509f0.021
15.0	16.31f0.10	-0.623f0.047	-0.495f0.023

Table II

The predicted results of three different five-point measurements of the W-pair threshold. Scan 1 is optimized for the measurement of M_W. Scan 2 is an attempt to improve the measurement of Γ_W. Scan 3 is identical to the threshold scan used in Reference 3. The results are presented for several assumptions about the level of residual background B and the W-pair detection efficiency.

Quantity	Scan 1	Scan 2	Scan 3
L[-5 GeV] (pb^{-1})	85	85	100
L[-1 GeV] (pb^{-1})	0	55	100
LIO GeV] (pb^{-1})	55	0	100
L[0.5 GeV] (pb^{-1})	55	55	0
L[1 GeV] (pb^{-1})	55	55	100
L[15 GeV] (pb^{-1})	250	250	100
B = 1.0 pb . $[2M_W]^2$ ε_{ww} = 0.53			
Number of Events	2951	2912	1863
δM_W (MeV)	160	176	150
$\delta\Gamma_W$ (MeV)	531	482	492
δB (pb . $[2M_W]^2$)	0.12	0.12	0.12
B = 0.5 pb . $[2M_W]^2$ ε_{ww} = 0.53			
Number of Events	2737	2698	1627
δM_W (MeV)	137	154	130
$\delta\Gamma_W$ (MeV)	50s	450	44s
δB (pb . $[2M_W]^2$)	0.096	0.09s	0.09s
B = 1.0 pb . $[2M_W]^2$ ε_{ww} = 0.70			
Number of Events	3760	3709	2309
δM_W (MeV)	130	144	123
$\delta\Gamma_W$ (MeV)	453	407	410
δB (pb · $[2M_W]^2$)	0.12	0.13	0.13

FIGURE CAPTIONS

1) The cross section for the process $e^+e^- \rightarrow f\bar{f}(\gamma)$ is plotted as a function of the normalized $f\bar{f}$ longitudinal momentum x_F and of the $f\bar{f}$ center-of-mass energy $E_{f\bar{f}}$. The center-of-mass energy of the e^+e^- system is 160 GeV.

2) The cross section for the process $e^+e^- \rightarrow W^+W^-$ as a function of $E_b - M_W$. The mass and width of the W are assumed to be SO GeV and 2.1 GeV, respectively. Note that three curves are plotted: the dashed curve is the basic tree-level cross section; the dashed-dotted curve is the cross section including the effect of initial state radiation; and the solid curve is the cross section including initial state radiation and the effect of a finite W width.

3) The sensitivity function for M_W as a function of the single beam energy about the W pair threshold $E_b - M_W$.

4) The sensitivity function for Γ_W as a function of the single beam energy about the W pair threshold $E_b - M_W$.

5) The sensitivity function for the background parameter B as a function of the single beam energy about the W pair threshold $E_b - M_W$.

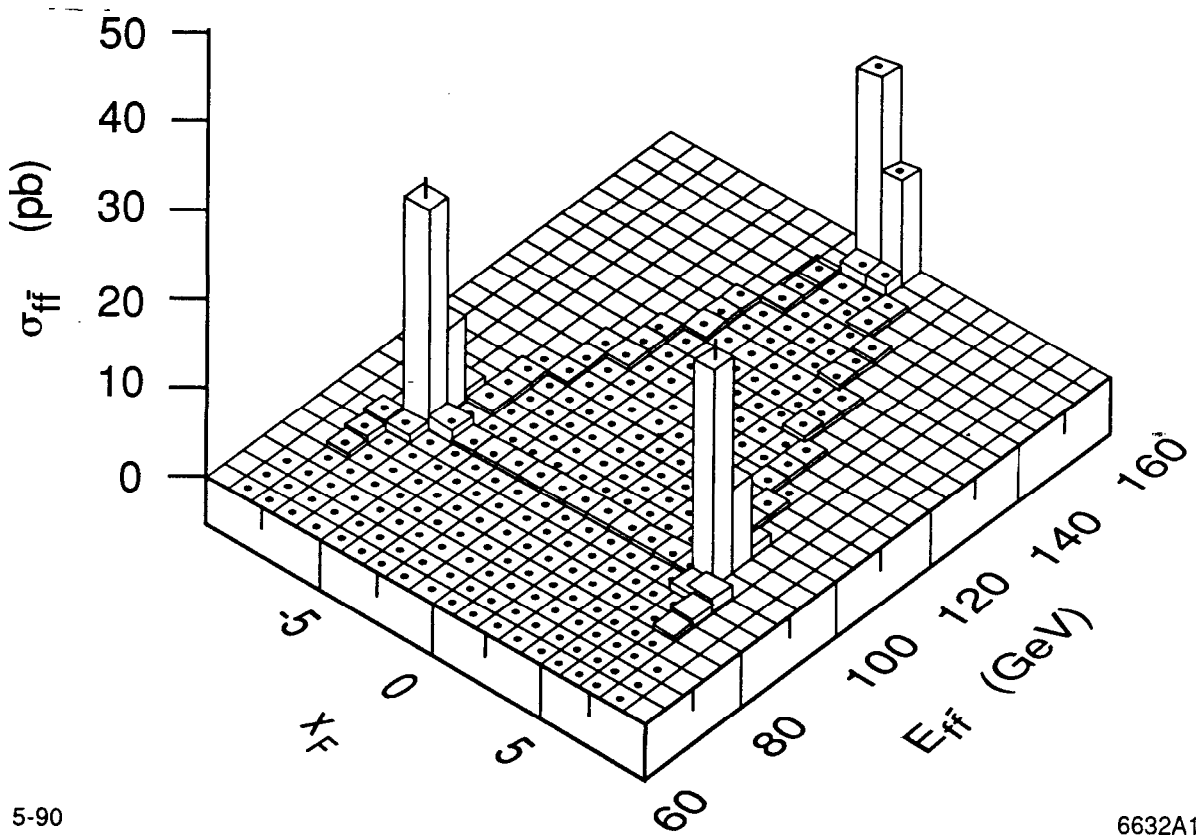
50
40
30
20
10
0
σ_{ff} (pb)
5
0
5
x_F
60
80
100
120
140
160
E_{ff} (GeV)
5-90
6632A1

Fig. 1

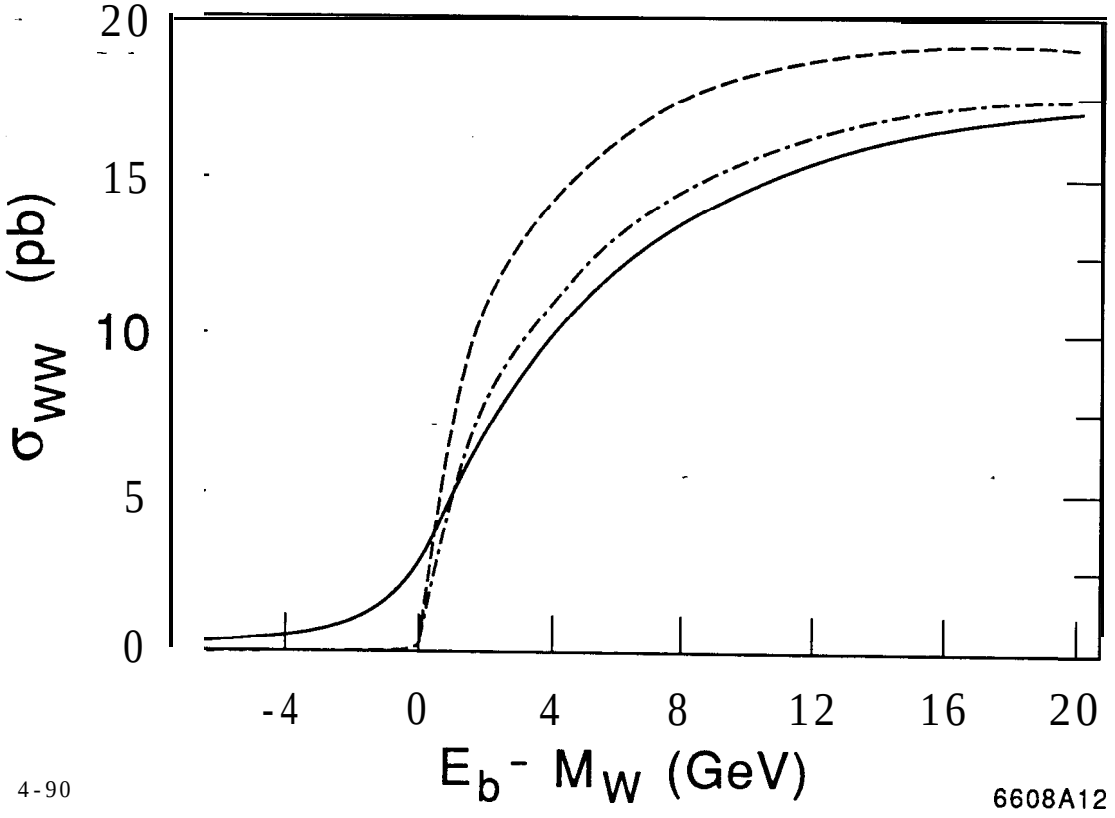

Fig. 2

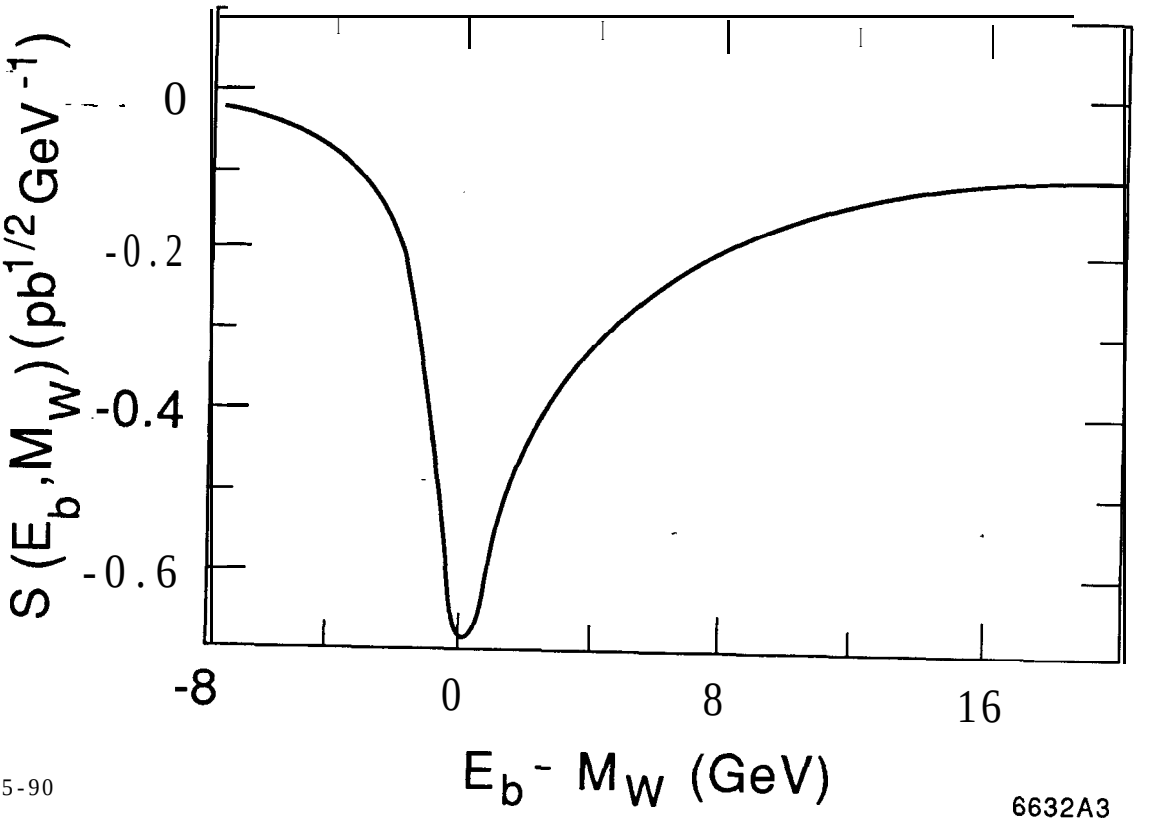

Fig. 3

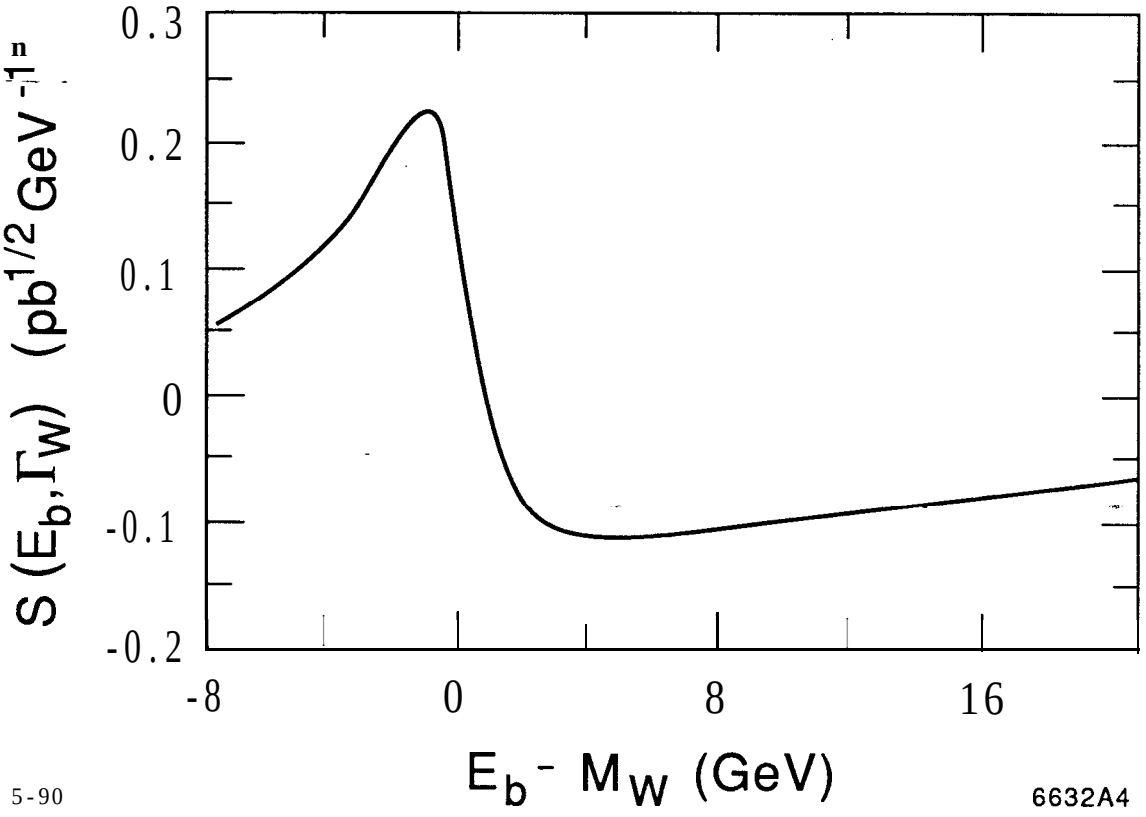

Fig. 4

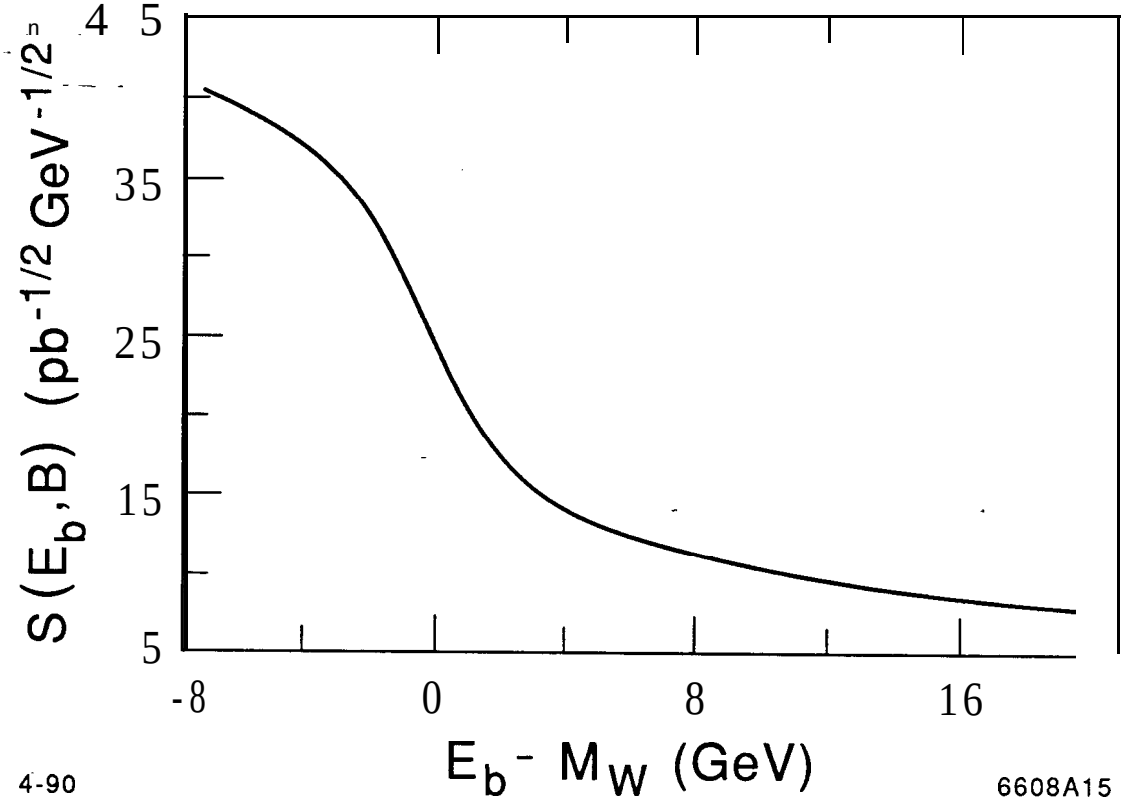

Fig. 5

Appendix A

The form of the cross section $\sigma(s, s_1, s_2)$ is reproduced from Reference 4 as follows,

$$\sigma(s, s_1, s_2) = \sigma_{AA} + \sigma_{ZZ} + \sigma_{\nu\nu} + \sigma_{AZ} + \sigma_{A\nu} + \sigma_{Z\nu},$$

where the partial cross sections are:

$$\sigma_{AA} = \frac{1}{64\pi s^2}\frac{e^4}{s^2}\left(-\frac{2}{s_1 s_2}\right) G_1(s, s_1, s_2),$$

$$\sigma_{ZZ} = \frac{1}{64\pi s^2}\frac{g^4}{16}\frac{v^2 + a^2}{(s - M_Z^2)^2}\left(-\frac{2}{s_1 s_2}\right) G_1(s, s_1, s_2),$$

$$\sigma_{\nu\nu} = \frac{1}{64\pi s^2}\frac{g^4}{8}\left(-\frac{2}{s_1 s_2}\right) G_2(s, s_1, s_2),$$

$$\sigma_{AZ} = \frac{1}{64\pi s^2}\frac{e^2 g^2}{2}\frac{\mathrm{v}}{s(s - M_Z^2)}\left(-\frac{2}{s_1 s_2}\right) G_1(s, s_1, s_2),$$

$$\sigma_{A\nu} = \frac{1}{64\pi s^2}\frac{e^2 g^2}{2}\frac{1}{s}\frac{2}{s_1 s_2} G_3(s, s_1, s_2),$$

$$\sigma_{Z\nu} = \frac{1}{64\pi s^2}\frac{g^4}{8}\frac{v - a}{s - M_Z^2}\frac{2}{s_1 s_2} 3(\%\ s_1, s_2).$$

The constants v and a are the vector and axial-vector couplings of the electron to the Z^0,

$$\mathrm{v} = 1 - 4\sin^2\theta_w$$

$$a = -1.$$

The functions G_1, G_2 and G_3 are given as follows:

$$G_1 = -\lambda^{3/2}(s, s_1, s_2)\{\lambda(s, s_1, s_2)/6 + 2[s(s_1 + s_2) + s_1 s_2]\},$$

$$G_2 = -\lambda^{1/2}(s, s_1, s_2)\{\lambda(s, s_1, s_2)/6 + 2[s(s_1 + s_2) - 4s_1 s_2]\}$$
$$+ 4s_1 s_2(s - s_1 - s_2)\ln[f(s, s_1, s_2)],$$

$$G_3 = -\lambda^{1/2}(s, s_1, s_2)\,[(s + 11s_1 + 11s_2)\lambda(s, s_1, s_2)/6$$
$$+ 2(s_1^2 + 3s_1 s_2 + s_2^2)s - 2(s_1^3 + s_2^3)]$$
$$- 4s_1 s_2[s(s_1 + s_2) + s_1 s_2]\ln[f(s, s_1, s_2)],$$

and the auxiliary functions λ and f are defined as,

$$\lambda(s, s_1, s_2) = s^2 + s_1^2 + s_2^2 - 2(s_1 s + s_2 s + s_1 s_2),$$
$$f(s, s_1, s_2) = \frac{s - s_1 - s_2 - \lambda^{1/2}(s, s_1, s_2)}{s - s_1 - s_2 + \lambda^{1/2}(s, s_1, s_2)}.$$

The W-pair cross section $\sigma(s, s_1, s_2)$ is sensitive to the weak coupling constant g and is relatively insensitive to the parameter $\sin^2 \theta_w$. At tree-level, the parameters g and $\sin^2 \theta_w$ can be expressed in terms of M_W as follows,

$$g^2 = 4\sqrt{2} G_F M_W^2$$
$$\sin^2 8, = A^2/M_W^2.$$

The precise measurement of M_Z has, in principle, fixed g and $\sin^2$ 0, except for loop-level corrections. If we assume that the Standard Model is correct, the M_W dependence of these quantities is much smaller than the tree-level expressions indicate. The full set of electroweak radiative corrections for $\sigma(s, s_1, s_2)$ is necessary to understand the M_W dependence.

For testing the Standard Model, it may not be desirable to use M_Z-constrained expressions for g and $\sin^2 \theta_w$. The parameters appearing in $\sigma(s, s_1, s_2)$ can be expressed as functions of M_W or allowed to vary as free parameters.

To investigate these effects, we have calculated the mass derivative $\partial\sigma_{ww}/\partial M_W$ for two cases:

1. The parameters g and $\sin^2 \theta_w$ are fixed to reasonable values (g = 0.65 and $\sin^2 \theta_w$ = 0.230).
2. The parameters g and $\sin^2 \theta_w$ are allowed to vary with M_W according to the tree-level expressions (about 0.65 and 0.230).

Although one might expect the M_W sensitivity of the second procedure to exceed that of the first, *the magnitude of the derivative $\partial\sigma_{ww}/\partial M_W$ is smaller in the second case (by $\sim$10% at its peak value).* This occurs because the presence of

the threshold causes σ_{ww} to decrease with increasing M_W and the weak coupling causes it to increase with increasing M_W. The use of the second fitting procedure would increase the errors δM_W listed in Table II by approximately 10%.

In the case that g is allowed to vary as a free parameter, the M_W derivative is equal to the fixed-g case. A fifth scan energy is then essential (our hypothetical scans do contain five points: four threshold points and one high energy point).